

1
2
3 1 **ALTERNATIVE ANALYSIS OF TRANSIENT INFILTRATION EXPERIMENT TO**
4
5 2 **ESTIMATE SOIL WATER REPELLENCY**
6
7 3

8 4 *Alagna V.¹, Iovino M.^{1*}, Bagarello V.¹, Mataix-Solera J.², Lichner E.³*
9
10 5

11 6 ¹ Dipartimento di Scienze Agrarie, Alimentari e Forestali, Università degli Studi di Palermo,
12 7 Palermo, Italy

13 8 ² Departamento de Agroquímica y Medio Ambiente, Universidad Miguel Hernández, Elche, Spain

14 9 ³ Institute of Hydrology, Slovak Academy of Sciences, Bratislava, Slovak Republic

15 10 Correspondence: M. Iovino, E-mail: massimo.iovino@unipa.it
16
17
18
19
20
21
22
23
24
25
26
27
28
29
30
31
32
33
34
35
36
37
38
39
40
41
42
43
44
45
46
47
48
49
50
51
52
53
54
55
56
57
58
59
60

12 Running head: Soil water repellency estimation from transient infiltration tests

14 Keywords: Infiltration, Soil sorptivity, Soil water repellency, Minidisk infiltrometer, Repellency
15 index, Two-term infiltration model, Water drop penetration time, Soil hydraulic conductivity.

Abstract

The repellency index (RI) defined as the adjusted ratio between soil-ethanol, S_e , and soil-water, S_w , sorptivities estimated from minidisk infiltrometer (MDI) experiments has been used instead of the widely used Water Drop Penetration Time (WDPT) and Molarity of Ethanol Drop (MED) tests to assess soil water repellency (SWR). However, sorptivity calculated by the usual early-time infiltration equation may be overestimated as the effects of gravity and lateral capillary are neglected. With the aim to establish the best applicative procedure to assess RI, different approaches to estimate S_e and S_w were compared that make use of both the early-time infiltration equation (namely, the one-minute, S1, and the short-time linearization, SL, approaches), and the two-term axisymmetric infiltration equation, valid for early to intermediate times (namely, the cumulative linearization, CL, and differentiated linearization, DL, approaches). The dataset included 85 MDI tests conducted in three sites in Italy and Spain under different vegetation habitats (forest of *Pinus pinaster* and *Pinus halepensis*, burned pine forest, annual grasses), soil horizons (organic and mineral), post-fire treatments and initial soil water contents. The S1 approach was inapplicable in 42% of experiments as water infiltration did not start in the first minute. The SL approach yielded a systematic overestimation of S_e and S_w that resulted in an overestimation of RI by a factor of 1.57 and 1.23 as compared with the CL and DL approaches. A new repellency index, RI_s , was proposed as the ratio between the slopes of the linearized data for the wettable and hydrophobic stages obtained by a single water infiltration test. For the experimental conditions considered, RI_s was significantly correlated with RI and WDPT. Compared to RI, RI_s includes information on both soil sorptivity and hydraulic conductivity and, therefore, it can be considered more physically linked to the hydrological processes affected by SWR.

Introduction

Soil water repellency (SWR) reduces affinity of soils to water resulting in detrimental implication for plant growth as well as for hydrological processes. These include reduced matrix infiltration, development of fingered flow, irregular wetting fronts, and overall increased runoff generation and soil erosion (DeBano, 2000; Doerr, Shakesby, & Walsh, 2000). During the last decades, it has become clear that SWR is much more widespread than formerly thought, having been reported for a wide variety of soils, land uses and climatic conditions (Dekker, Oostindie, & Ritsema, 2005). Soil water repellency stems from re-orientation of amphiphilic compounds during heating or drying which results in a non-zero contact angle between water and soil. In severe cases, when the contact angle exceeds 90° , water infiltration is prevented (Letey, Carrillo, & Pang, 2000). However, it has

1
2
3 50 increasingly been recognized that infiltration rates and pattern can be affected by “sub-critical”
4
5 51 repellency that occurs when the water-solid contact angle is less than 90° but not zero (Tillman,
6
7 52 Scotter, Wallis, & Clothier, 1989). Under these circumstances, water infiltration rate is reduced but
8
9 53 not prevented at all, as in the case of severe hydrophobicity (Hunter, Chau, & Si, 2011).

10 54 Due to its dynamic nature, including dependence on the initial soil water content, testing of
11
12 55 SWR should be conducted directly under field-moist samples (Dekker, Ritsema, Oostindie, Moore,
13
14 56 & Wesseling, 2009). The water drop penetration time (WDPT) test (Doerr, 1998; Letey et al., 2000;
15
16 57 Watson & Letey, 1970) has been diffusely applied to assess the persistence of SWR. However,
17
18 58 WDPT is a measure of the time required for the contact angle to change from its original value,
19
20 59 which can be greater than 90° , to a value approaching 90° (Cerdà & Doerr, 2007; Letey et al.,
21
22 60 2000). Given the wettability of a hydrophobic soil surface can be increased by lowering the surface
23
24 61 tension of the liquid, the severity of SWR can be assessed by using different mixtures of water and
25
26 62 ethanol. With the Molarity of an Ethanol Droplet (MED) test, the severity of SWR is associated to
27
28 63 the concentration (or liquid–air surface tension) of the aqueous ethanol solution that enters the soil
29
30 64 in approximately 5 s (Letey et al., 2000). However, the MED test can only be used to determine
31
32 65 apparent contact angles $>90^\circ$ and thus only to discriminate between critical and subcritical SWR
33
34 66 (Carrillo, Yates, & Letey, 1999; Müller et al., 2016). Independently of the considered test (i.e.,
35
36 67 WDPT or MED), the soil surface area sampled in a drop scale infiltration test is of the order of 0.14
37
38 68 cm^2 and SWR assessment can be significantly influenced by spatial variability (Moody &
39
40 69 Schlossberg, 2010).

41 70 Tillman et al. (1989) proposed a repellency index, RI, to assess sub-critical SWR that
42
43 71 basically is a measure of the reduced soil water sorptivity compared to a non-repellent soil. Given
44
45 72 ethanol readily infiltrates into hydrophobic soil, its sorptivity provides a measure of liquid transport
46
47 73 in soil that is not influenced by SWR and is representative of pore structure (Orfánus et al., 2014).
48
49 74 RI is defined as the ratio between soil-ethanol, S_e , and soil-water, S_w , sorptivities adjusted to
50
51 75 account for the different surface tensions and viscosities of the two infiltrating liquids
52
53 76 ($\text{RI}=1.95 \cdot S_e/S_w$) (Tillman et al., 1989). Iovino et al. (2018) proposed a classification of RI similar to
54
55 77 that for WDPT with five classes of repellency considered: wettable ($\text{RI} \leq 1.95$); slightly water
56
57 78 repellent ($1.95 \leq \text{RI} < 10$); strongly water repellent ($10 \leq \text{RI} < 50$); severely water repellent ($50 \leq \text{RI}$
58
59 79 < 110) and extremely water repellent ($\text{RI} \geq 110$). Compared with drop scale infiltration tests, RI is
60
61 80 determined from infiltration tests conducted at a larger scale and, thus, take into account soil
62
63 81 properties and conditions (e.g., initial soil moisture, geometry and connectivity of pores) that
64
65 82 directly influence the effects of SWR on hydrological processes. Tension infiltration experiments
66
67 83 are preferred to ponded ones to exclude the contribution of macropores that may overwhelm soil

1
2
3 84 hydrophobicity (Ebel, Moody, & Martin, 2012; Nyman, Sheridan, & Lane, 2010). Miniaturized
4
5 85 tension infiltrometers were proposed to determine SWR at the aggregate scale (Hallett & Young,
6
7 86 1999) but, for field use, standard infiltrometers are more suited. Hunter et al. (2011) compared the
8
9 87 influence of tension infiltrometer disk size on the measured RI values and concluded that the
10 88 minidisk infiltrometer (MDI) (Decagon Devices Inc., Pullman, USA), having a 4.5 cm diameter
11
12 89 disk, is appropriate for field assessment of RI. In a recent investigation, the MDI proved to be a
13
14 90 practical alternative to the classical tension infiltrometer to estimate hydrodynamic properties of a
15 91 loam soil (Alagna, Bagarello, Di Prima, & Iovino, 2016).

16
17 92 Soil sorptivity, S_0 ($L T^{-0.5}$), is commonly estimated from the Philip (1957) horizontal
18
19 93 infiltration equation, but the assessment of the linear part of cumulative infiltration, I (L), vs. square
20
21 94 root of time, t (T), relationship describing the early stage of the infiltration process could be
22
23 95 relatively problematic in water repellent soils (Carrick, Buchan, Almond, & Smith, 2011; Di Prima,
24 96 Lassabatere, Bagarello, Iovino, & Angulo-Jaramillo, 2016). Sorptivity was estimated as the
25
26 97 infiltration rate out of a MDI during a fixed time interval, generally 1-5 min (Hunter et al., 2011;
27
28 98 Lewis, Wu, & Robichaud, 2006; Robichaud, Lewis, & Ashmun, 2008), as it is considered fast
29
30 99 enough to be an operational procedure for teams working in the field. However, the early-time
31
32 100 linear regression of the I vs. \sqrt{t} data neglects the effects of gravity and lateral capillary flux at the
33
34 101 edge of the source thus resulting in S_0 overestimation (Angulo-Jaramillo, Bagarello, Iovino, &
35
36 102 Lassabatere, 2016). An unbiased estimation of soil sorptivity is possible by fitting the two-term
37
38 103 cumulative infiltration equation proposed by Haverkamp, Ross, Smettem, and Parlange (1994) to
39
40 104 the infiltration data collected from early to intermediate infiltration times. In this case, validity of
41
42 105 Philip's equation is not needed (Bagarello & Iovino, 2003; Vandervaere, Vauclin, & Elrick, 2000a).
43
44 106 The Haverkamp et al. (1994) model has been largely applied to estimate the hydrodynamic
45
46 107 properties of a variety of soils using infiltration data collected under both tension and ponded
47
48 108 conditions (Bagarello, Di Prima, Iovino, & Provenzano, 2014; Dohnal, Dusek, & Vogel, 2010;
49
50 109 Gonzalez-Sosa et al., 2010). However, to the best of our knowledge, the two-term infiltration model
51
52 110 has never been applied to assess SWR.

53
54 111 Determination of the repellency index needs two sorptivity values, one for water and the other
55
56 112 for ethanol, to be determined. As a consequence of the influence of the initial soil water content on
57
58 113 both ethanol and water sorptivity (Tillman et al., 1989), the two experiments cannot be conducted at
59
60 114 exactly the same spot. Due to both horizontal and vertical spatial variability of SWR (e.g., Dekker,
61
62 115 Doerr, Oostindie, Ziogas, & Ritsema, 2001), a large number of replicated runs should be carried out
63
64 116 to obtain a reliable estimate of the repellency index, for a given area, by the ratio of the averages of
65
66 117 sorptivity found with ethanol and water. The possibility to derive a repellency index from a unique

1
2
3 118 water infiltration experiment conducted by the MDI at a single spot is thus intriguing, also
4
5 119 considering the potential advantages that stem from the simplicity of the technique (portability,
6
7 120 small volumes of water, short duration of field experiment). An attempt to assess SWR by a single
8
9 121 experiment was made by Lichner et al. (2013) who defined the water repellency cessation time
10 122 (WRCT) as the time corresponding to the intersection of the two straight lines representing the I vs.
11
12 123 \sqrt{t} relationship for hydrophobic and near wettable conditions. Alagna, Iovino, Bagarello, Mataix-
13
14 124 Solera, and Lichner (2017) found that the WRCT was significantly correlated to WDPT and
15 125 concluded that WRCT is essentially a measure of the persistence of SWR. However, the potentiality
16
17 126 of a single water infiltration experiment conducted with the MDI to provide information on the
18
19 127 SWR still needs investigation also because water repellent and wettable soils could show
20
21 128 qualitatively similar behaviours when infiltration data are reported on a I vs. \sqrt{t} plot (Cook &
22
23 129 Broeren, 1994; Smettem, Parlange, Ross, & Haverkamp, 1994).

24 130 The general objective of this study was to strengthen the techniques for assessing SWR from
25
26 131 tension infiltration experiments conducted in the field by the MDI. In particular, with the aim to
27
28 132 establish the best applicative procedure to estimate the classical water repellency index according to
29
30 133 Tillman et al. (1989), different techniques to calculate the soil sorptivity using ethanol, S_e , and
31 134 water, S_w , were compared including i) infiltration rate in a fixed time interval, ii) analysis of early-
32
33 135 time infiltration data and iii) linearization of the axisymmetric transient infiltration equation. With
34
35 136 the aim to simplify SWR assessment, a new repellency index, obtained from a unique water
36 137 infiltration test, was proposed and evaluated with existing approaches. Three Mediterranean sites
37
38 138 under various soil/vegetation/management conditions were considered to evaluate the different
39
40 139 procedures for estimating SWR.

41 140

42 141

43 142

44 143

45 144

46 145

47 146

48 147

49 148

50 149

51 150

52 151

53 152

54 153

55 154

56 155

57 156

58 157

59 158

60 159

Theory

Haverkamp et al. (1994) proposed the following three-dimensional infiltration equation for disk infiltrimeters, valid for short to medium times:

$$I = S_0 \sqrt{t} + \left[\frac{2 - \beta}{3} K_0 + \frac{\gamma S_0^2}{r(\theta_0 - \theta_i)} \right] t \quad (1)$$

where I (L) is the cumulative infiltration, t (T) is the infiltration time, θ_0 ($L^3 L^{-3}$) is the volumetric soil water content corresponding to the imposed pressure head at the soil surface, h_0 (L), θ_i ($L^3 L^{-3}$) is the initial volumetric soil water content, $S_0 = S(h_0)$ ($L T^{-1/2}$) is the soil sorptivity, $K_0 = K(h_0)$ ($L T^{-1}$) is the soil hydraulic conductivity, r (L) is the radius of the disk source and β and γ are coefficients

that are commonly set at 0.6 and 0.75, respectively. The first term of the right-hand side of eq. (1) accounts for vertical capillary flow and dominates infiltration during its early stage. The second term corresponds to the gravity-driven vertical flow and the third one represents the lateral capillary component at the edge of the circular infiltration surface (Smettem et al., 1994).

Eq. (1) can be linearized by dividing both sides by \sqrt{t} (Cumulative Linearization, CL, method) or by differentiating the cumulative infiltration data with respect to the square root of time (Differentiated Linearization, DL, method) (Vandervaere et al., 2000a). In both cases, the soil sorptivity can be estimated as the intercept of the regression line fitted to the linearized experimental data. With this approach, the effects of gravity and lateral expansion are explicitly accounted for and soil sorptivity can be obtained using the complete experimental information collected for short to medium time (Angulo-Jaramillo et al., 2016). Vandervaere, Vauclin, and Elrick (2000b) proposed the DL method to account for the water stored in the contact material during the early stages of infiltration. However, if no contact material is used, the CL and DL methods should result in similar S_0 estimates. A test of the expected equivalence of the two methods was conducted by Bagarello and Iovino (2004) who found that the two linearization methods were not perfectly equivalent in estimating S_0 . When the experimental cumulative infiltration data are plotted in the form of I/\sqrt{t} vs. \sqrt{t} or $dI/d\sqrt{t}$ vs. \sqrt{t} , the validity of eq. (1) can easily be checked and discontinuities in the infiltration process can easily be detected given they result in deviation from the monotonically increasing linear behaviour (Vandervaere et al., 2000a). Water repellency is one of most common circumstances producing deviation from the classical infiltration theory (Di Prima et al., 2016; Ebel & Moody, 2013; Imeson, Verstraten, van Mulligen, & Sevink, 1992).

In water repellent soils, infiltration rate can be expected to increase, after an initial stage at null or low values, as a consequence of soil wetting (Beatty & Smith, 2013; Carrick et al., 2011). Therefore, comparing the soil hydrodynamic data collected during the initial hydrophobic and subsequent wetting stages of an infiltration process potentially allows us to quantify SWR. In particular, provided eq. (1) can separately be applied to both stages, the extent of water repellency can be defined as the ratio, RI_s , between the slopes of the linearized cumulative infiltration relationships fitting the hydrophobic and wetting stages of the infiltration process corresponding to an imposed h_0 value:

$$RI_s = \frac{\left[\frac{2-\beta}{3} K_{ws} + \frac{\gamma S_{ws}^2}{r \Delta \theta} \right]}{\left[\frac{2-\beta}{3} K_{rs} + \frac{\gamma S_{rs}^2}{r \Delta \theta} \right]} \quad (2)$$

in which the subscript ws refers to the wetting stage of infiltration, the subscript rs refers to the repellent stage, and $\Delta \theta = \theta_0 - \theta_l$ (**figure 1**). For wettable soils a value $RI_s = 1$ is expected.

1
2
3 182 Compared to repellency indices that make use of two sorptivity measurements conducted with
4
5 183 ethanol and water at two different sites, the repellency index defined by eq. (2) needs only one
6
7 184 infiltration experiment with water at a single spot and it accounts for the effects induced by water
8
9 185 repellency on the two hydrodynamic properties (sorptivity and hydraulic conductivity) that directly
10 186 influence the hydrological processes.

11 12 187 13 14 188 **Materials and methods**

15 189 Field sites

16
17 190 Infiltration data were collected in the two Mediterranean managed pine forests of Ciavolo (Italy)
18
19 191 and Javea (Spain), already investigated by Alagna et al. (2017), and in the fire-affected forest site of
20
21 192 Javea, in which different post-fire management strategies were implemented. Soil at Ciavolo site is
22 193 a *Typic Rhodoxeralf* (Soil Survey Staff, 2014) and the forest consists of 30 years old *Pinus pinaster*
23
24 194 trees. Measurements were conducted on both the approximately 5-cm thick decomposed organic
25
26 195 floor layer (duff) and the underlying mineral soil layer two times in 2014 (in summer and autumn)
27
28 196 to explore different moisture conditions (Alagna et al., 2017). Indeed, influence of initial soil
29 197 moisture on water repellency is well recognized in literature (i.e., de Jonge, Jacobsen, & Moldrup,
30
31 198 1999; Dekker et al., 2001; Vogelmann et al., 2013). Between the two measurement times, 108 mm
32
33 199 of rainfall occurred that is approximately 20% of the average annual precipitation for the location.
34 200 For comparative purposes, a glade area vegetated with spontaneous annual grasses (*Avena fatua* L.,
35
36 201 *Galactites elegans* (All.) Soldano, *Hypochaeris achyrophorus* L., *Oxalis pes-caprae* L. and *Vulpia*
37
38 202 *ciliata* Dumort) was also sampled, approximately 50 m away from the pine site, at the second
39
40 203 measurement time. Only the surface mineral layer was sampled at this site given that a well-
41 204 developed organic layer was not detectable. Average air temperature on the two sampling dates was
42
43 205 24.7 °C and 18.2 °C, respectively.

44
45 206 The second measurement site is located at Javea close to Alicante, Spain, in a 40-years old
46 207 afforested plantation of *Pinus halepensis* that was settled on abandoned agricultural terraces. The
47
48 208 soil is *Lithic Rhodoxeralf* (Soil Survey Staff, 2014) developed over a karstified limestone.
49
50 209 Measurements were conducted in the beginning of July 2015 at the surface duff and the underlying
51
52 210 mineral soil layer. The mean air temperature at the time of measurements was 26.5 °C and no
53 211 rainfall had occurred in the three months prior to sampling thus resulting in relatively dry initial soil
54
55 212 moisture conditions.

56
57 213 The third site was also located at Javea in an area that was fire-affected in September 2014
58 214 resulting in a complete loss of forest trees. Starting from December 2014, the following two
59
60 215 alternative post-fire management strategies were implemented in this area: i) burned trees were cut

1
2
3 216 at the ground level and removed (cutting treatment, C) and, ii) the soil was mulched with chopped
4
5 217 pine residues (residue treatment, R). For comparative purposes, a control plot (no treatment, N), in
6
7 218 which no operation was performed and the burned vegetation was left in situ, was also considered.
8
9 219 Field measurements at the three plots of the fire-affected site were performed on 15-17 June 2015.
10 220 Only the soil mineral layer was sampled after removing ash and/or mulching residues. The mean
11
12 221 daily temperature at the time of sampling was 20.8° C. Characteristics of experimental sites were
13
14 222 summarized in **table 1**.

15 223 For the aim of comparisons among repellency indices calculated by the different procedures,
16
17 224 ten experimental conditions were therefore considered resulting from different habitats (i.e., *Pinus*
18
19 225 *pinaster* forest in Ciavolo (P), spontaneous annual grasses in Ciavolo (G), *Pinus halepensis* forest in
20 226 Javea (H), burned pine forest in Javea (B)), sampled horizons (i.e., organic (O) or mineral (M)),
21
22 227 climatic conditions at the vegetated sites (i.e., dry (D) or wet (W) season) and post-fire treatments at
23
24 228 the fire-affected site (no treatment (N), cutting treatment (C), and residues treatment (R)). Each
25
26 229 experimental condition is therefore identified by three capital letters indicating, respectively,
27 230 habitat, sampled horizon and soil moisture at the time of sampling or post-fire treatment.
28

29 231 Field measurements

30
31 232 For each experimental condition, a flat area (approximately 5 x 5 m²) was selected and scrubbed
32 233 soil samples were randomly collected in the first 5 cm of each sampled horizon to determine
33 234 particle size distribution (PSD), using the hydrometer method (Gee & Bauder, 1986), and organic
34 235 matter (OM) content by the Walkley-Black method (Nelson & Sommers, 1996). The clay, silt and
35 236 sand percentages were determined, as a mean of three replicated samples, according to USDA
36 237 standards (**table 1**). Undisturbed soil cores were randomly collected by gently pressing stainless
37 238 steel cylinders (0.05 m in height by 0.05 m in diameter) into the sampled soil layer to determine soil
38 239 bulk density, ρ_b (Mg m⁻³), and volumetric water content at the time of sampling, θ_i (m³m⁻³) (**table**
39 240 **2**).
40
41 241

42 242 The water drop penetration time (WDPT) test was carried out under field moist conditions by
43 243 placing 30 drops of deionized water in different smoothed locations within the sampling area from a
44 244 standard height of 10 mm and recording the time for their complete penetration. A medical dropper
45 245 was used that yielded drops of uniform volume ($70 \pm 5 \mu\text{L}$). According to Hallin, Douglas, Doerr,
46 246 and Bryant (2013), the applied protocol allows estimating the mean WDPT value with an error of
47 247 $\pm 10\%$ at 95% confidence. Five classes of repellency were considered: wettable (WDPT ≤ 5 s);
48 248 slightly water repellent ($5 < \text{WDPT} \leq 60$ s); strongly water repellent ($60 < \text{WDPT} \leq 600$ s); severely
49
50
51
52
53
54
55
56
57
58
59
60

1

2

3 249 water repellent ($600 < \text{WDPT} \leq 3600$ s) and extremely water repellent ($\text{WDPT} > 3600$ s) (Bisdorn,
4 Dekker, & Schoute, 1993; Dekker et al., 2009).

6

7 251 For each experimental condition, five to ten infiltration tests were conducted by a standard
8 252 MDI with a 45 mm diameter disk and an imposed pressure head at the soil surface $h_0 = -2$ cm. Both
9 253 95% ethanol and deionized water were used, placing the disk of the MDI directly on the soil surface
10 254 previously levelled using a spatula without adding or removing material from the infiltration spot.
11 255 When necessary, soil depressions were filled by small amount of 2-mm sieved soil collected near
12 256 the infiltration point. Infiltration spot preparation was therefore considered to not affect SWR
13 257 estimation. A stand and a clamp were used to maintain the MDI upright. Approximately 50 mm of
14 258 ethanol or water was allowed to infiltrate in each MDI test. Overall, 85 infiltration tests with ethanol
15 259 and 85 infiltration tests with water were conducted at the experimental sites. Cumulative infiltration
16 260 of ethanol was visually recorded at the MDI reservoir at intervals of 10 s for the first minute, every
17 261 30 s for the successive two minutes and, finally, every one minute until the complete infiltration of
18 262 the prescribed volume (approximately 0.08 L, corresponding to a cumulative infiltration $I = 50$
19 263 mm). Infiltration of water was much slower than infiltration of ethanol and, therefore, measurement
20 264 intervals were increased up to 15 min. For 14 runs, the infiltration process was stopped before the
21 265 MDI reservoir had completely emptied but, in any case, test duration was at least 3 h. Only for the
22 266 15 runs conducted with water at the fire-affected site of Javea, infiltration runs were stopped after
23 267 1.5 h when average cumulative infiltration was 27.5 mm (0.044 L). This circumstance did not
24 268 preclude application of eq. (2) to calculate RI_s . The depth of the wetting front, as detected by soil
25 269 excavation at the end of the infiltration test, was generally limited to 4-5 cm.

39

40 270 Soil sorptivity using water, S_w , and ethanol, S_e , was estimated by different approaches: 1) $S =$
41 271 I_1/\sqrt{t} , I_1 being the cumulative infiltration in the first minute of the run (one-minute approach, S1);
42 272 2) slope of the straight line describing the I vs. \sqrt{t} relationship during the early stage of the
43 273 infiltration process according to Philip (1957) (short-time linearization approach, SL); 3) intercept
44 274 of the regression line fitting the linearized infiltration data in the form of I/\sqrt{t} vs. \sqrt{t} (cumulative
45 275 linearization approach, CL); and 4) intercept of the regression line fitting the linearized infiltration
46 276 data in the form of $dI/d\sqrt{t}$ vs. \sqrt{t} (differentiated linearization approach, DL).

51

52 277 To exclude influence of soil spatial variability on RI estimation, the procedure proposed by
53 278 Pekarova, Pekar, and Lichner (2015) was applied by considering all the possible combinations of
54 279 estimated S_e and S_w values within an experimental site (i.e., 100 estimates of RI were obtained at the
55 280 forest and grass sites of Ciavolo and Javea and 25 estimates at burned forest site of Javea).
56 281 According to the different approaches, four RI datasets were obtained for each experimental
57 282 condition (i.e., RI_{S1} , RI_{SL} , RI_{CL} , RI_{DL}). For each MDI test conducted with water ($N = 85$), a RI_s

60

value was calculated by eq. (2) using the linearized cumulative infiltration data in the form of CL (RI_{s-CL}) and DL (RI_{s-DL}) approaches.

According to the findings by Alagna et al. (2017), a log-normal distribution was considered for RI , RI_s and $WDPT$ whereas a normal distribution was considered for other datasets (Coutinho et al., 2016; Di Prima et al., 2016). Mean and coefficient of variation (CV) of a given dataset were calculated according to the associated statistical distribution (Lee, Reynolds, Elrick, & Clothier, 1985). Comparisons between two mean values were conducted by a paired t-test, whereas comparisons among three mean values by a Tukey highly significant difference (HSD) test. In both cases, a significance level of 0.05 was considered.

Results and Discussion

MDI tests with ethanol

Cumulative infiltration of ethanol was in line with the infiltration theory given that a transient phase, in which infiltration rate decreased, was followed by a steady state infiltration phase in which infiltration rate was practically constant (**figure 2a**). In most cases, the I vs. t relationships appeared linear, with no concavity or a concavity limited to the very early stage of infiltration. This linear trend indicated that gravity and lateral capillary influenced the axisymmetric flow out of the disk source very soon after the beginning of the infiltration process (Bagarello, Ferraris, & Iovino, 2004; Di Prima et al., 2016; Dohnal et al., 2010; Vandervaere et al., 2000a, 2000b).

Steady state infiltration rate, i_s ($L T^{-1}$), determined by the least-squares regression slope of the linear portion of the I vs. t curve (Bagarello, Iovino, & Reynolds, 1999), ranged between 45.1 and 1065 $mm h^{-1}$ ($CV = 80.9\%$) and the minimum and maximum i_s values were obtained for the organic soil at the pine forest sites of Javea (H-O-D) and Ciavolo (P-O-D), respectively, thus showing the large variability of conditions that may be encountered under a similar type of vegetation. The mean steady state infiltration rates were generally higher in the clay-loam soil of Ciavolo (P and G habitats) than in the sandy-loam and silt-clay soils of Javea (B and H habitats) (**table 3**).

Limiting the analysis to the mineral soils (i.e., neglecting the organic soils for consistency among the three datasets collected at the different experimental sites), the steady state infiltration rates decreased in the order: Ciavolo clay-loam (175 - 293 $mm h^{-1}$, depending on the habitat) > Javea sandy-loam (107 - 167 $mm h^{-1}$) > Javea silty-clay (101 $mm h^{-1}$). Due to different surface tension and density of ethanol, the effective applied pressure head at the soil surface was -5 cm (Jarvis, Etana, & Stagnitti, 2008). As smaller conductive pores are more frequent in fine textured

1
2
3 316 soils than in coarse textured porous media (e.g., Hillel, 1998), a higher value of i_s in the clay-loam
4
5 317 soil is not uncommon.

6
7 318 The time required to achieve steady state flow, t_s (T) (Bagarello et al., 1999), was larger than
8
9 319 the fixed time to estimate sorptivity according to the S1 approach ($t = 1$ min) in 95.3% of cases.
10 320 Therefore, obtaining steady-state flow required more than 1 min and thus a transient phase
11
12 321 potentially usable to estimate sorptivity by both the S1 and SL approaches was available. As a
13
14 322 matter of fact, plots of I vs. \sqrt{t} showed an initial linear part including at least four data points, thus
15 323 allowing reliable estimates of soil sorptivity according to the SL approach. Mean values of ethanol
16
17 324 sorptivity estimated according to the S1 and SL approaches for the different experimental
18
19 325 conditions spanned over a similar range of values (**table 3**) and the S_e values estimated by the two
20
21 326 approaches for each MDI test ($N = 85$) were highly correlated (**figure 3a**). However, a bias from the
22 327 identity line was observed for high sorptivity values denoting that the influence of lateral capillary,
23
24 328 and probably of gravity, comes into play even for time lower than 1 min. According to a paired t-
25
26 329 test ($P = 0.05$), the two approaches were not equivalent in estimating S_e (**table 3**).

27
28 330 A linear relationship between I/\sqrt{t} and \sqrt{t} (CL approach) and between $dI/d\sqrt{t}$ and \sqrt{t} (DL
29
30 331 approach) was visually recognized for the entire duration of the infiltration test in most cases (77%
31 332 and 79%, respectively). In the remaining cases, a definite linear trend including at least 50% of the
32
33 333 cumulative infiltration data was detected thus suggesting that both approaches were always
34
35 334 applicable. Applicability of eq.(1) was statistically assessed by calculating the coefficients of
36 335 determination, R^2 , for the I/\sqrt{t} vs. \sqrt{t} and $dI/d\sqrt{t}$ vs. \sqrt{t} linear regressions. In particular, R^2
37
38 336 values for each infiltration test were always significant ($P = 0.05$) and higher than 0.629 for the CL
39
40 337 approach (mean $R^2 = 0.977$) and 0.513 (mean $R^2 = 0.859$) for the DL approach. Mean S_e values
41
42 338 estimated by the CL and DL approaches were not significantly different (**table 3**) and the regression
43 339 line between the single S_e estimates obtained by the two approaches ($N = 84$) was not different from
44
45 340 the identity line (**figure 3b**). However, mean S_e values obtained by the experimental information
46
47 341 collected from early to intermediate infiltration time (CL and DL approaches) were lower than those
48
49 342 obtained using only the early time information (**table 3**). Therefore, the four considered approaches
50 343 for estimating ethanol sorptivity were not equivalent and a systematic overestimation of S_e was
51
52 344 observed for the approaches (S1 and SL) that make use of early-time infiltration data only. This
53
54 345 result makes the choice to calculate S_e using only infiltration data collected in the early stage of the
55 346 infiltration process questionable.

56
57 347
58
59 348 MDI tests with water
60

1
2
3 349 Plots of cumulative water infiltration vs. time typically exhibited an upward convex shape that is
4
5 350 indicative of water repellency occurrence (**figure 2b**). In particular, the increase in infiltration rates
6
7 351 with time suggests a reduction in SWR as infiltration proceeds (Beatty & Smith, 2013; Carrick et
8
9 352 al., 2011; Di Prima et al., 2016; Ebel & Moody, 2013; Imeson et al., 1992). Prolonged contact with
10 353 water can lead to the loss of SWR as a consequence of the changes in orientation of amphiphilic
11
12 354 molecules on a mineral surface while in contact with water (Doerr et al., 2000). The WDPT test
13
14 355 (Van't Woudt, 1959), for example, is a measure of the duration of this process which depends on a
15 356 variety of biotic and abiotic factors and leads to a wettable soil and, thus, to an increase in
16
17 357 infiltration rate.

18
19 358 Due to hydrophobicity, the time needed for total water volume to infiltrate ($I = 50$ mm) was
20
21 359 much longer than with ethanol ranging up to 9 h (**table 4**). Mean values of the infiltration rate \bar{v} , i.e.
22 360 the ratio between the final cumulative volume and the corresponding duration, were lower for the
23
24 361 organic soils ($3.8 \leq \bar{v} \leq 12.6$ mm h⁻¹) than mineral soils ($17.5 \leq \bar{v} \leq 126.6$ mm h⁻¹) (**table 4**). The
25
26 362 highest \bar{v} values were obtained in the glade site of Ciavolo (G-M-W) ($\bar{v} = 101.7$ mm h⁻¹) and in the
27 363 mineral subsoil of the pine forest in Javea (H-M-D) ($\bar{v} = 126.6$ mm h⁻¹).

28
29 364 The very slow infiltration in the early stages of the process made the estimation of soil water
30
31 365 sorptivity, S_w , problematic. Indeed, in 36 infiltration tests conducted with water (42% of cases),
32
33 366 water flow out of the MDI did not start during the first minute of infiltration, making it impossible
34
35 367 to estimate S_w by the S1 approach. Wetting of soil surface, as detected by the rising of the first air
36 368 bubble within the MDI reservoir, was particularly slow in the organic soil of the pinus forests (P-O-
37
38 369 D, P-O-W, H-O-D), where the average time for the start of infiltration was 705 s (maximum value =
39
40 370 3000 s). For the remaining 49 runs, the S_w values calculated by the S1 approach ranged from 5.1 to
41 371 76.4 mm h^{-0.5}, with a mean value of 18.0 mm h^{-0.5} (CV = 93.8%). According to a paired t-test ($P =$
42
43 372 0.05), mean S_w estimated from the same experimental dataset by the S1 approach was higher than
44
45 373 the sorptivity estimated by the remaining three approaches (SL, CL and DL) (**table 4**).

46 374 Despite the difficulties in detecting the start of the wetting process, analysis of water
47
48 375 infiltration data confirmed the results obtained with ethanol as infiltrating fluid. A criterion based
49
50 376 on a fixed short time (1 min in this case) tended to overestimate both ethanol and water sorptivity
51
52 377 whereas, in extremely water repellent soils, it was not appropriate for assessing the initial stage of
53 378 infiltration. Therefore, its application as a general criterion for assessing repellency is questionable.
54
55 379 Maybe, the poor applicability of S1 approach in strongly hydrophobic soils could be overcome by
56
57 380 selecting a shorter time interval for ethanol infiltration and a larger time interval for water
58
59 381 infiltration but this choice appears arbitrary and would probably hinder the benefit of rapidity and
60 382 simplicity for which this approach has been proposed (Lewis et al., 2006; Robichaud et al., 2008).

1
2
3
4
5
6
7
8
9
10
11
12
13
14
15
16
17
18
19
20
21
22
23
24
25
26
27
28
29
30
31
32
33
34
35
36
37
38
39
40
41
42
43
44
45
46
47
48
49
50
51
52
53
54
55
56
57
58
59
60

383 Due to this drawback, the S1 approach was excluded from the subsequent analysis on the
384 assessment of SWR.

385 The CL and DL approaches could not be applied in five and three cases out of 85,
386 respectively, as it was not possible to identify a monotonic increasing trend in the I/\sqrt{t} vs. \sqrt{t} or
387 $dI/d\sqrt{t}$ vs. \sqrt{t} data or the intercept of the regression line was negative. The SL, CL and DL
388 approaches yielded statistically equivalent estimates of S_w (**table 4**) even if an overestimation of
389 sorptivity was detected when only early time infiltration data were used (SL approach) (**figure 4**).
390 For water infiltration tests, gravity and lateral capillary probably came into play at a later stage of
391 the infiltration process as compared with the ethanol infiltration tests and, therefore, the SL
392 approach did not result in S_w overestimation similar to those detected, by the same approach, for S_e .
393 The S_w values estimated by the linearization approaches (i.e., CL and DL) were not significantly
394 different (**table 4**) and the linear regression line between the individual S_w estimates was not
395 different from the identity line (confidence intervals for intercept and slope: $-1.29 - 0.22$, $0.91 -$
396 1.01 , respectively) (**figure 4**).

398 Classical repellency index

399 Independently of the estimation approach (SL, CL or DL), mean S_e values for each experimental
400 condition (**table 3**) were higher than the corresponding S_w values (**table 4**), the only exception being
401 for the mineral soil of the pine forest of Javea (H-M-D) in which non-repellent conditions were
402 clearly observed during field tests. Estimation of the repellency index according to the classical
403 procedure by Tillman et al. (1989) depended on the approach followed to estimate S_e and S_w (**table**
404 **5**). According to a Tukey HSD test, discrepancies between the RI values calculated with different
405 sorptivity estimation approaches (i.e., RI_{SL} , RI_{CL} and RI_{DL}) tended to be less pronounced in
406 hydrophobic soils than in less water repellent soils. Depending on the experimental condition, the
407 ratio RI_{SL}/RI_{CL} ranged between 0.93 and 3.24, whereas RI_{SL}/RI_{DL} was in the range 0.51-2.11. On
408 average, RI_{SL} overestimated SWR, as compared to RI_{CL} and RI_{DL} by a factor of 1.57 and 1.23,
409 respectively (**table 5**). In eight out of ten experimental conditions, RI_{CL} and RI_{DL} were not
410 statistically different. This was an expected result given that the S_e and S_w values estimated by the
411 two approaches were not statistically different (**table 3 and 4**) and the scatterplots of S_e and S_w were
412 close to the 1:1 line (**figures 3b and 4b**). In 70% of the cases, RI_{SL} differed from those calculated
413 by one or both alternative approaches and most of the differences occurred since the SL approach
414 yielded higher SWR estimation than the CL and/or DL approaches. Therefore, the SL approach for
415 estimating ethanol and water sorptivities may result in RI overestimation, particularly under low
416 SWR conditions.

1
2
3 417 The two approaches based on the linearization of the cumulative infiltration curve yielded
4
5 418 generally similar estimates of RI and can therefore be considered equally usable for field estimation
6
7 419 of SWR. Moreover, these estimates of RI could be expected to be reliable since they are based on
8
9 420 an approach that distinguishes among the different forces driving infiltration. However, a negative
10 421 aspect of using linearization approaches is that S estimation may be affected by a subjective
11
12 422 selection of the linear part of the I/\sqrt{t} vs. \sqrt{t} and $dI/d\sqrt{t}$ vs. \sqrt{t} plots to be used for fitting eq.
13
14 423 (1) to the data (Bagarello & Iovino, 2004; Vandervaere et al., 2000a, 2000b). In general, selection
15 424 of data describing a linearly increasing relationship was easier on the CL than the DL plot due to the
16
17 425 scattering effect associated to the finite difference calculation of the term $dI/d\sqrt{t}$ (**figure 5**).
18

19 426 The RI value for H-M-D was lower than 1.95 (**table 5**) which was considered by Tillman et
20
21 427 al. (1989) as the value discriminating between non-repellent and repellent conditions. It is worth
22
23 428 noting that the RI values were always higher in the surface organic horizons than in the underlying
24 429 mineral ones with values ranging up to $RI = 55$ under dry conditions. However, relatively high RI
25
26 430 values were also observed in the mineral horizon of the pine forest of Ciavolo (P-M-D and P-M-W)
27
28 431 and also in the burned site of Javea mulched with chopped pine residues (B-M-R) (**table 5**). As
29 432 highlighted by Alagna et al. (2017), leaching of hydrophobic compound from the overlying organic
30
31 433 duff or mulching layer could be responsible for these findings.
32

33 434 34 435 *New repellency index*

36 436 The total cumulative water infiltration data, linearized in the form of either CL or DL approaches,
37
38 437 always showed an increasing trend that was characterized by a practically unique slope in non-
39
40 438 repellent soils (**figure 5b and 5d**) and, conversely, showed a typical “hockey-stick-like” shape in
41
42 439 water repellent soils (**figure 5a and 5c**). In the latter case, the experimental plot was characterized
43 440 by an initial increasing linear part followed, after a knee, by a more or less pronounced increase in
44
45 441 slope. Independently of the shape of the linearized plot, the slopes for the initial and the later stages
46
47 442 of the infiltration processes were calculated. Identification was easy in 94% of the cases for the CL
48 443 approach and in 80% of the cases when the DL approach was considered. In one case only, the two
49
50 444 approaches were not applicable. In the remaining cases (i.e., 6% of cases for CL and 20% for DL),
51
52 445 the estimation of one of the two slopes was characterized by a very small number of points (i.e.,
53
54 446 three points), or a low, non-significant coefficient of correlation was found. Nevertheless, a
55 447 meaningful trend was always visually detectable and, therefore, these estimations were maintained
56
57 448 in the dataset.

58
59 449 The mean RI_s values calculated by the CL and DL approaches were not statistically different
60 450 in eight out of ten experimental conditions (**table 6**) and the regression line between the RI_{s-CL} and

1

2

3 451 RI_{s-DL} was characterized by a significant $R^2 = 0.9663$ and was not different from the identity line
4
5 452 (confidence intervals for intercept and slope: $-1.26 - 3.17$, $0.87 - 1.18$, respectively). Depending on
6
7 453 the considered experimental condition, the RI_{s-CL} values ranged from 1.2 to 37.9 and the RI_{s-DL} from
8
9 454 1.7 to 39.3 (**table 6**). The clear increasing trend of RI_s at increasing soil hydrophobicity was
10 455 confirmed by the significant correlations that were found, independently of the approach (CL or
11
12 456 DL), with the classical RI and WDPT indices (**table 7**). In particular, the new RI_s index detected
13
14 457 repellency condition for the mineral soil of the glade at Ciavolo (G-M-W) ($RI_s = 2.3-2.7$) that was
15 458 classified as not repellent according to the traditional WDPT test (mean water drop penetration time
16
17 459 < 5 s). This result was in line with RI values that ranged between 1.7 and 2.7 (**table 5**), thus
18
19 460 confirming that the RI_s index can be able to detect slight SWR conditions that could be not assessed
20
21 461 by the commonly used WDPT classification (Bisdorn et al., 1993; Dekker et al., 2009). On the other
22 462 hand, inconsistency between WDPT and RI or RI_s was observed for the organic layer of Javea
23
24 463 forest site (H-O-D) that was severely water repellent according to the WDPT test ($t = 2139$ s) but
25
26 464 slightly water repellent according to the RI and RI_s tests (**figure 6**). As a consequence of this
27
28 465 discrepancy, the coefficients of determination for RI_{s-CL} vs. WDPT and RI_{s-DL} vs. WDPT linear
29 466 regressions were low despite still significant ($P = 0.05$) (**table 7**). When the point corresponding to
30
31 467 this experimental condition was excluded from the regression analysis, the coefficient of
32
33 468 determination increased up to $R^2 = 0.8803$ ($P = 0.01$) for RI_{s-CL} vs. WDPT linear regression and R^2
34 469 $= 0.8943$ ($P = 0.01$) for RI_{s-DL} vs. WDPT one. Despite WDPT and RI_s explore different soil
35
36 470 volumes and, thus, are probably not fully comparable, testing the new proposed RI_s with available
37
38 471 and well-assessed technique, like WDPT, is the only viable approach to assess its reliability.
39
40 472 Comparisons between infiltration based repellency indices and WDPT were conducted, among
41 473 others, by Bughici and Wallach (2016); Lewis et al. (2006) and Schacht, Chen, Tarchitzky, Lichner,
42
43 474 and Marschner (2014). The significant correlation found under different
44
45 475 soil/vegetation/management conditions is encouraging and supports the conclusion that the
46
47 476 information gathered from a single water infiltration experiment conducted by the MDI for a
48 477 relatively long time interval is potentially exploitable to assess SWR.

49

50 478 Similar conclusions were drawn by Lichner et al. (2013) who proposed to assess the soil
51
52 479 hydrophobicity by the water repellency cessation time (WRCT) that was estimated as the
53
54 480 intersection between the two regression lines representing the early-time (hydrophobic) and late-
55 481 time (wetttable) conditions when the cumulative infiltration data are plotted on a I vs. \sqrt{t} plot. The
56
57 482 new proposed RI_s was significantly correlated with WRCT calculated according to Lichner et al.
58
59 483 (2013) ($R^2=0.8385$ for RI_{s-CL} vs. WRCT linear regression and $R^2=0.8466$ for RI_{s-DL} vs. WRCT one).
60 484 For the reduced dataset collected only at the forested sites of Ciavolo and Javea, Alagna et al.

(2017) also tested a modified repellency index, RI_m , defined as the ratio of the slopes of the I vs. \sqrt{t} plot at the late and early stages of the infiltration process (Sepehrnia, Hajabbasi, Afyuni, & Lichner, 2016). However, both the WRCT and the RI_m are obtained from the I vs. \sqrt{t} plot of cumulative water infiltration data. The new repellency index RI_s seems to be more physically robust than WRCT and RI_m indices as these two approaches neglect the influence of gravity and lateral capillary that comes into play after the very early-time stage of the infiltration process. Actually, plots of I vs. \sqrt{t} may exhibit an upward convex shape that is not due to increased soil wettability as infiltration proceeds but depends on the progressively increasing importance of gravity and lateral capillary flow (Cook & Broeren, 1994; Smettem, Ross, Haverkamp, & Parlange, 1995). Using cumulative infiltration data in the form of I vs. \sqrt{t} plot may thus misestimate the repellency phenomena. In **figure 7**, for two ethanol tests, infiltration data are plotted in I vs. \sqrt{t} form and according to CL and DL linearization approaches. As can be seen, CL and DL plots (**figure 7b and 7c**) are clearly linear, as they should be for ethanol infiltration, whereas I vs. \sqrt{t} plot shows an increasing slope that might be attributed to an artefact water repellency that is not real in fact. On the other hand, the repellency index calculated according to eq. (2) includes information on both sorptivity and conductivity measured in the wettable and repellent stages of the infiltration process and, therefore, it can be considered more directly linked to the hydrological processes affected by soil water repellency.

Conclusions

The adjusted ratio between ethanol and water sorptivities, estimated by a tension infiltration experiment, is a valuable tool to assess the extent of SWR. However, the commonly applied horizontal infiltration equation that makes use only of the initial stage of the axisymmetric flow out of a MDI may result in overestimations of sorptivity due to the neglected effects of gravity and lateral capillary on infiltration. The two-term infiltration model proposed by Haverkamp et al. (1994), that is valid for early to intermediate infiltration times, is potentially more able to yield unbiased estimations of sorptivity. For variable experimental conditions resulting from different soil texture, vegetation habitat, sampled horizon, soil management and initial water content, the approaches based on the linearization of the two-term infiltration model (CL and DL) yielded similar estimates of S_e and S_w . A systematic overestimation of S_e was observed with approaches (S1 and SL) that make use of early-time infiltration data only. Moreover, the S1 approach was inapplicable in 42% of experiments conducted with water, thus preventing estimation of the repellency index, RI, proposed by Tillman et al. (1989). The biases in S_e and S_w estimations obtained by the SL approach yielded an overestimation of RI by a factor of 1.57 and 1.23 as

1
2
3 519 compared to the values estimated with the CL and DL approaches. Moreover, these discrepancies
4
5 520 were more pronounced in less water repellent soils.

6 521 For the experimental conditions considered, the mean values of the new repellency index, the
7
8 522 RI_s , defined as the ratio of the slopes of the linearized cumulative infiltration data in the wettable
9
10 523 and repellent stages of infiltration, were significantly correlated with the mean RI and WDPT
11
12 524 indices thus showing the potential reliability of soil hydrophobicity assessment by this index.
13
14 525 Compared to the RI index, RI_s is estimated from a single water infiltration experiment conducted by
15 526 the MDI, as well as other tension infiltrometers, thus overcoming drawbacks of conducting paired
16
17 527 water and ethanol infiltration experiments in two different spots (i.e., small scale spatial variability,
18
19 528 variable temperature effect on the physical characteristics of the two infiltrating liquids). As for
20
21 529 previously proposed repellency indices (i.e., WRCT, RI_m), the new RI_s offers a way to quantify with
22 530 a single number the complex site-specific soil wetting properties. However, RI_s appears physically
23
24 531 more sound in that it includes information on both sorptivity and hydraulic conductivity measured
25
26 532 in the early repellent and subsequent wettable stages of the infiltration process thus being more
27 533 directly linked to the hydrological processes affected by soil water repellency.

28
29 534 Further investigations are necessary to test the validity of the new index on different SWR
30
31 535 conditions also with the aim to define classification criteria more quantitatively associated to the
32
33 536 actual water-solid contact angle.

34 537
35

36 538 **Acknowledgements**

37
38 539 This study was supported by grants from the Università degli Studi di Palermo (Dottorato di
39 540 Ricerca in Scienze Agrarie, Forestali e Ambientali, ciclo XXIX, D50002D13+1012), Ministero
40
41 541 dell'Istruzione, dell'Università e della Ricerca (PRIN 2015 project GREEN4WATER no.
42
43 542 B72F16000550005), the Slovak Research and Development Agency APVV (project No. APVV-15-
44
45 543 0160), Ministerio de Economía and Competitividad of Spanish Government (project CGL2013-
46 544 47862-C2-1-R), Botánica Mediterránea S.L., and Montgó Natural Park. Field data in Italy and
47
48 545 Spain were collected by V. Alagna. All authors analyzed the data and contributed to write the
49
50 546 manuscript.

51 547
52

53 548
54

55 549 **References**

56 550 Alagna, V., Bagarello, V., Di Prima, S., & Iovino, M. (2016). Determining hydraulic properties of a
57
58 551 loam soil by alternative infiltrometer techniques. *Hydrological Processes*, 30(2), 263-275.
59
60 552 doi:10.1002/hyp.10607

- 1
2
3 553 Alagna, V., Iovino, M., Bagarello, V., Mataix-Solera, J., & Lichner, L. (2017). Application of
4
5 554 minidisk infiltrometer to estimate water repellency in Mediterranean pine forest soils. *Journal*
6
7 555 *of Hydrology and Hydromechanics*, 65(3), 254-263. doi:10.1515/johh-2017-0009
8
9 556 Angulo-Jaramillo, R., Bagarello, V., Iovino, M., & Lassabatere, L. (2016). Unsaturated soil
10 557 hydraulic properties. *Infiltration Measurements for Soil Hydraulic Characterization* (pp. 181-
11
12 558 287). Cham: Springer International Publishing.
13
14 559 Bagarello, V., Di Prima, S., Iovino, M., & Provenzano, G. (2014). Estimating field-saturated soil
15 560 hydraulic conductivity by a simplified Beerkan infiltration experiment. *Hydrological*
16
17 561 *Processes*, 28(3), 1095-1103. doi:10.1002/hyp.9649
18
19 562 Bagarello, V., Ferraris, S., & Iovino, M. (2004). An evaluation of the single-test tension
20
21 563 infiltrometer method for determining the hydraulic conductivity of lateral capillarity domain
22 564 Soils. *Biosystems Engineering*, 87(2), 247-255. doi:http://dx.doi.org/10.1016/
23
24 565 j.biosystemseng.2003.11.007
25
26 566 Bagarello, V., & Iovino, M. (2003). Field testing parameter sensitivity of the two-term infiltration
27 567 equation using differentiated linearization. *Vadose Zone Journal*, 2(3), 358-367.
28
29 568 doi:10.2136/vzj2003.3580
30
31 569 Bagarello, V., & Iovino, M. (2004). Indagine di laboratorio su una metodologia innovativa per la
32
33 570 determinazione della conducibilità idraulica del suolo con l'infiltrometro a depressione.
34 571 *Rivista di Ingegneria Agraria*, 35(2), 81-92.
35
36 572 Bagarello, V., Iovino, M., & Reynolds, W. D. (1999). Measuring hydraulic conductivity in a
37
38 573 cracking clay soil using the Guelph Permeameter. *Transactions of the ASAE*, 42(4), 957-964.
39
40 574 Beatty, S. M., & Smith, J. E. (2013). Dynamic soil water repellency and infiltration in post-wildfire
41 575 soils. *Geoderma*, 192, 160-172. doi:http://dx.doi.org/10.1016/j.geoderma.2012.08.012
42
43 576 Bisdom, E. B. A., Dekker, L. W., & Schoute, J. F. T. (1993). Water repellency of sieve fractions
44
45 577 from sandy soils and relationships with organic material and soil structure. *Geoderma*, 56(1),
46 578 105-118. doi:https://doi.org/10.1016/0016-7061(93)90103-R
47
48 579 Bughici, T., & Wallach, R. (2016). Formation of soil–water repellency in olive orchards and its
49
50 580 influence on infiltration pattern. *Geoderma*, 262,1-11. doi:https://doi.org/10.1016/j.geoderma.
51 581 2015.08.002
52
53 582 Carrick, S., Buchan, G., Almond, P., & Smith, N. (2011). Atypical early-time infiltration into a
54
55 583 structured soil near field capacity: The dynamic interplay between sorptivity, hydrophobicity,
56
57 584 and air encapsulation. *Geoderma*, 160(3–4), 579-589. doi:http://dx.doi.org/10.1016/
58 585 j.geoderma.2010.11.006
59
60

- 1
2
3 586 Carrillo, M. L. K., Yates, S. R., & Letey, J. (1999). measurement of initial soil-water contact angle
4 of water repellent soils. *Soil Science Society of America Journal*, 63(3), 433-436.
5 587
6 588 doi:10.2136/sssaj1999.03615995006300030002x
- 8 589 Cerdà, A., & Doerr, S. H. (2007). Soil wettability, runoff and erodibility of major dry-
9 Mediterranean land use types on calcareous soils. *Hydrological Processes*, 21(17), 2325-
10 590 2336. doi:10.1002/hyp.6755
11 591
- 13 592 Cook, F. J., & Broeren, A. (1994). Six methods for determining sorptivity and hydraulic
14 conductivity with disk permeameters. *Soil Science*, 157(1), 2-11.
15 593
- 17 594 Coutinho, A. P., Lassabatere, L., Montenegro, S., Antonino, A. C. D., Angulo-Jaramillo, R., &
18 Cabral, J. J. S. P. (2016). Hydraulic characterization and hydrological behaviour of a pilot
19 595 permeable pavement in an urban centre, Brazil. *Hydrological Processes*, 30(23), 4242-4254.
20 596
21 597 doi:10.1002/hyp.10985
22 598
- 24 598 DeBano, L. F. (2000). Water repellency in soils: a historical overview. *Journal of Hydrology*, 231-
25 232(0), 4-32. doi:http://dx.doi.org/10.1016/S0022-1694(00)00180-3
26 599
- 27 600 de Jonge, L. W., Jacobsen, O. H., & Moldrup, P. (1999). Soil water repellency: effects of water
28 content, temperature, and particle size. *Soil Science Society of America Journal*, 63(3), 437-
29 601 442. doi:10.2136/sssaj1999.03615995006300030003x
30 602
- 32 603 Dekker, L. W., Doerr, S. H., Oostindie, K., Ziogas, A. K., & Ritsema, C. J. (2001). Water
33 repellency and critical soil water content in a dune sand. *Soil Science Society of America
34 604 Journal*, 65(6), 1667-1674. doi:10.2136/sssaj2001.1667
35 605
- 37 606 Dekker, L. W., Oostindie, K., & Ritsema, C. J. (2005). Exponential increase of publications related
38 to soil water repellency. *Australian Journal of Soil Research*, 43(3), 403-441.
39 607
40 608 doi:10.1071/SR05007
41 609
- 43 609 Dekker, L. W., Ritsema, C. J., Oostindie, K., Moore, D., & Wesseling, J. G. (2009). Methods for
44 determining soil water repellency on field-moist samples. *Water Resources Research*, 45.
45 610
46 611 doi:Artn W00d3310.1029/2008wr007070
47 612
- 48 612 Di Prima, S., Lassabatere, L., Bagarello, V., Iovino, M., & Angulo-Jaramillo, R. (2016). Testing a
49 new automated single ring infiltrometer for Beerkan infiltration experiments. *Geoderma*, 262,
50 613 20-34. doi:http://dx.doi.org/10.1016/j.geoderma.2015.08.006
51 614
- 53 615 Doerr, S. H. (1998). On standardizing the 'Water Drop Penetration Time' and the 'Molarity of an
54 Ethanol Droplet' techniques to classify soil hydrophobicity: A case study using medium
55 616 textured soils. *Earth Surface Processes and Landforms*, 23(7), 663-668.
56 617
57 618 doi:10.1002/(SICI)1096-9837(199807)23:7<663::AID-ESP909>3.0.CO;2-6
58 619
59 600

- 1
2
3 619 Doerr, S. H., Shakesby, R. A., & Walsh, R. P. D. (2000). Soil water repellency: its causes,
4 characteristics and hydro-geomorphological significance. *Earth-Science Reviews*, 51(1–4),
5 620 33-65. doi:http://dx.doi.org/10.1016/S0012-8252(00)00011-8
6 621
7
8 622 Dohnal, M., Dusek, J., & Vogel, T. (2010). Improving hydraulic conductivity estimates from
9 minidisk infiltrometer measurements for soils with wide pore-size distributions. *Soil Science
10 623 Society of America Journal*, 74(3), 804. doi:10.2136/sssaj2009.0099
11 624
12
13 625 Ebel, B. A., & Moody, J. A. (2013). Rethinking infiltration in wildfire-affected soils. *Hydrological
14 626 Processes*, 27(10), 1510-1514. doi:10.1002/hyp.9696
15
16
17 627 Ebel, B. A., Moody, J. A., & Martin, D. A. (2012). Hydrologic conditions controlling runoff
18 generation immediately after wildfire. *Water Resources Research*, 48. doi:Artn W0352910.
19 628 1029/2011wr011470
20 629
21
22 630 Gee, G. W., & Bauder, J. W. (1986). Particle-size analysis. In A. Klute (Ed.), *Methods of Soil
23 631 Analysis, Part 1: Physical and Mineralogical Methods* (2nd ed., pp. 383-411). Madison, WI:
24 632 ASA- SSSA.
25
26
27 633 Gonzalez-Sosa, E., Braud, I., Dehotin, J., Lassabatere, L., Angulo-Jaramillo, R., Lagouy, M., . . .
28 634 Michel, K. (2010). Impact of land use on the hydraulic properties of the topsoil in a small
29 635 French catchment. *Hydrological Processes*, 24(17), 2382-2399. doi:Doi 10.1002/Hyp.7640
30
31
32 636 Hallett, P. D., & Young, I. M. (1999). Changes to water repellence of soil aggregates caused by
33 637 substrate-induced microbial activity. *European Journal of Soil Science*, 50(1), 35-40. doi:DOI
34 638 10.1046/j.1365-2389.1999.00214.x
35
36
37 639 Hallin, I., Douglas, P., Doerr, S. H., & Bryant, R. (2013). The role of drop volume and number on
38 640 soil water repellency determination. *Soil Science Society of America Journal*, 77(5), 1732-
39 641 1743. doi:10.2136/sssaj2013.04.0130
40
41
42 642 Haverkamp, R., Ross, P. J., Smettem, K. R. J., & Parlange, J. Y. (1994). 3-dimensional analysis of
43 643 infiltration from the disc infiltrometer. 2. Physically-based infiltration equation. *Water
44 644 Resources Research*, 30(11), 2931-2935. doi:Doi 10.1029/94wr01788
45
46
47 645 Hillel, D. (1998). *Environmental soil physics*. San Diego, CA: Academic Press.
48
49
50 646 Hunter, A. E., Chau, H. W., & Si, B. C. (2011). Impact of tension infiltrometer disc size on
51 647 measured soil water repellency index. *Canadian Journal of Soil Science*, 91(1), 77-81.
52 648 doi:10.4141/cjss10033
53
54
55 649 Imeson, A. C., Verstraten, J. M., van Mulligen, E. J., & Sevink, J. (1992). The effects of fire and
56 650 water repellency on infiltration and runoff under Mediterranean type forest. *Catena*, 19(3–4),
57 651 345-361. doi:http://dx.doi.org/10.1016/0341-8162(92)90008-Y
58
59
60

- 1
2
3 652 Iovino M., Pekárová P., Hallett P.D., Pekár J., Lichner L., Mataix-Solera J., ... Rodný M. (2018).
4
5 653 Extent and persistence of soil water repellency induced by pines in different geographic
6
7 654 regions. *Journal of Hydrology and Hydromechanics*, 66(4), 360-368. DOI: 10.2478/johh-
8
9 655 2018-0024
- 10 656 Jarvis, N., Etana, A., & Stagnitti, F. (2008). Water repellency, near-saturated infiltration and
11
12 657 preferential solute transport in a macroporous clay soil. *Geoderma*, 143(3–4), 223-230.
13
14 658 doi:http://dx.doi.org/10.1016/j.geoderma.2007.11.015
- 15 659 Lee, D. M., Reynolds, W. D., Elrick, D. E., & Clothier, B. E. (1985). A comparison of three field
16
17 660 methods for measuring saturated hydraulic conductivity. *Canadian Journal of Soil Science*,
18
19 661 65(3), 563-573.
- 20 662 Letey, J., Carrillo, M. L. K., & Pang, X. P. (2000). Approaches to characterize the degree of water
21
22 663 repellency. *Journal of Hydrology*, 231–232(0), 61-65. doi:http://dx.doi.org/10.1016/S0022-
23
24 664 1694(00)00183-9
- 25 665 Lewis, S. A., Wu, J. Q., & Robichaud, P. R. (2006). Assessing burn severity and comparing soil
26
27 666 water repellency, Hayman Fire, Colorado. *Hydrological Processes*, 20(1), 1-16.
28
29 667 doi:10.1002/hyp.5880
- 30
31 668 Lichner, L., Hallett, P. D., Drongová, Z., Czachor, H., Kovacik, L., Mataix-Solera, J., & Homolák,
32
33 669 M. (2013). Algae influence the hydrophysical parameters of a sandy soil. *Catena*, 108(0), 58-
34
35 670 68. doi:http://dx.doi.org/10.1016/j.catena.2012.02.016
- 36 671 Moody, D. R., & Schlossberg, M. J. (2010). Soil water repellency index prediction using the
37
38 672 molarity of ethanol droplet test. *Vadose Zone Journal*, 9(4), 1046-1051.
39
40 673 doi:10.2136/vzj2009.0119
- 41 674 Müller, K., Carrick, S., Meenken, E., Clemens, G., Hunter, D., Rhodes, P., & Thomas, S. (2016). Is
42
43 675 subcritical water repellency an issue for efficient irrigation in arable soils? *Soil and Tillage*
44
45 676 *Research*, 161, 53-62. doi:https://doi.org/10.1016/j.still.2016.03.010
- 46 677 Nelson, D. W., & Sommers, L. E. (1996). Total carbon, organic carbon and organic matter. In D. L.
47
48 678 Sparks, A. L. Page, P. A. Helmke, & R.H. Loeppert (Eds.), *Methods of soil analysis, Part 3,*
49
50 679 *Chemical methods* (pp. 961-1010). Madison, WI: Soil Science Society of America Inc.
- 51 680 Nyman, P., Sheridan, G., & Lane, P. N. J. (2010). Synergistic effects of water repellency and
52
53 681 macropore flow on the hydraulic conductivity of a burned forest soil, south-east Australia.
54
55 682 *Hydrological Processes*, 24(20), 2871-2887. doi:10.1002/hyp.7701
- 56
57 683 Orfánus, T., Dlapa, P., Fodor, N., Rajkai, K., Sándor, R., & Nováková, K. (2014). How severe and
58
59 684 subcritical water repellency determines the seasonal infiltration in natural and cultivated
60

1
2
3
4
5
6
7
8
9
10
11
12
13
14
15
16
17
18
19
20
21
22
23
24
25
26
27
28
29
30
31
32
33
34
35
36
37
38
39
40
41
42
43
44
45
46
47
48
49
50
51
52
53
54
55
56
57
58
59
60

- sandy soils. *Soil and Tillage Research*, 135, 49-59. doi:<https://doi.org/10.1016/j.still.2013.09.005>
- Pekarova, P., Pekar, J., & Lichner, L. (2015). A new method for estimating soil water repellency index. *Biologia*, 70(11), 1450-1455. doi:10.1515/biolog-2015-0178
- Philip, J. R. (1957). The theory of infiltration: 1. The Infiltration equation and its solution. *Soil Science*, 83(5), 345-358.
- Robichaud, P. R., Lewis, S. A., & Ashmun, L. E. (2008). New procedure for sampling infiltration to assess post-fire soil water repellency. *Res. Note*. RMRS-RN-33. Rocky Mountain Station US: Department of Agriculture, Forest Service.
- Schacht, K., Chen, Y., Tarchitzky, J., Lichner, L., & Marschner, B. (2014). Impact of treated wastewater irrigation on water repellency of Mediterranean soils. *Irrigation Science*, 32(5), 369-378. doi:10.1007/s00271-014-0435-3
- Sepehrnia, N., Hajabbasi, M. A., Afyuni, M., & Lichner, L. (2016). Extent and persistence of water repellency in two Iranian soils. *Biologia*, 71(10), 1137-1143. doi:10.1515/biolog-2016-0135
- Smettem, K. R. J., Parlange, J. Y., Ross, P. J., & Haverkamp, R. (1994). 3-dimensional analysis of infiltration from the disc infiltrometer. 1. A capillary-based theory. *Water Resources Research*, 30(11), 2925-2929. doi:10.1029/94wr01787
- Smettem, K. R. J., Ross, P. J., Haverkamp, R., & Parlange, J. Y. (1995). 3-dimensional analysis of infiltration from the disk infiltrometer. 3. Parameter-estimation using a double-disk tension infiltrometer. *Water Resources Research*, 31(10), 2491-2495. doi:10.1029/95wr01722
- Soil Survey Staff (2014). *Keys to Soil Taxonomy* (12th edition ed.). Washington, DC: USDA-NRCS.
- Tillman, R. W., Scotter, D. R., Wallis, M. G., & Clothier, B. E. (1989). Water-repellency and its measurement by using intrinsic sorptivity. *Australian Journal of Soil Research*, 27(4), 637-644. doi:10.1071/Sr9890637
- Vandervaere, J.-P., Vauclin, M., & Elrick, D. E. (2000a). Transient flow from tension infiltrometers. I. The two-parameter equation. *Soil Science Society of America Journal*, 64(4), 1263-1272. doi:10.2136/sssaj2000.6441263x
- Vandervaere, J.-P., Vauclin, M., & Elrick, D. E. (2000b). Transient flow from tension infiltrometers. II. Four methods to determine sorptivity and conductivity. *Soil Science Society of America Journal*, 64 (4), 1272-1284. doi:10.2136/sssaj2000.6441272x
- Van't Woudt, B. D. (1959). Particle coatings affecting the wettability of soils. *Journal of Geophysical Research*, 64(2), 263-267. doi:10.1029/JZ064i002p00263

1
2
3
4
5
6
7
8
9
10
11
12
13
14
15
16
17
18
19
20
21
22
23
24
25
26
27
28
29
30
31
32
33
34
35
36
37
38
39
40
41
42
43
44
45
46
47
48
49
50
51
52
53
54
55
56
57
58
59
60

- 718 Vogelmann, E. S., Reichert, J. M., Prevedello, J., Consensa, C. O. B., Oliveira, A. É., Awe, G. O.,
719 & Mataix-Solera, J. (2013). Threshold water content beyond which hydrophobic soils become
720 hydrophilic: The role of soil texture and organic matter content. *Geoderma*, 209–210(0), 177-
721 187. doi:<http://dx.doi.org/10.1016/j.geoderma.2013.06.019>
- 722 Watson, C. L., & Letey, J. (1970). Indices for Characterizing Soil-Water Repellency Based upon
723 Contact Angle-Surface Tension Relationships. *Soil Science Society of America Proceedings*,
724 34(6), 841-844. doi:10.2136/sssaj1970.03615995003400060011x

For Peer Review

1
2
3 **1 Figure captions**
4
5

6 3 Figure 1 – Selection of the water repellent and wetting stages from linearized infiltration data (CL
7 4 method).
8

9 5
10 6 Figure 2 – Example of cumulative infiltration curves obtained in selected sites using a) ethanol and
11 7 b) water as infiltrating fluid
12
13

14 8
15 9 Figure 3 – Comparison between ethanol sorptivity values, S_e , estimated according to different
16 10 approaches: a) SL vs. S1, b) CL vs. DL
17
18

19 11
20 12 Figure 4 – Comparison between water sorptivity values, S_w , estimated according to different
21 13 approaches: a) SL vs. CL, b) CL vs. DL
22
23

24 14
25 15 Figure 5 – Examples of application of cumulative linearization CL approach (a and b) and
26 16 differentiated linearization DL approach (c and d) to water infiltration experiments in hydrophobic
27 17 (a and c) and non-hydrophobic (b and d) soils
28
29

30 18
31 19 Figure 6 – Relationship between the repellency index RI_s calculated by the DL approach and the
32 20 Water Drop Penetration Time (WDPT) for the different experimental conditions considered ($N = 9$).
33 21 Filled dot refers to the data collected in the organic layer of Javea forest site (H-O-D) that was
34 22 excluded from the regression analysis.
35
36
37
38

39 23
40 24 Figure 7 – Examples of cumulative ethanol infiltration curves plotted according to different
41 25 representations: a) linearization of the early time infiltration data in the form I vs. $t^{0.5}$; b)
42 26 linearization of the complete infiltration curve according to CL approach; c) linearization of the
43 27 complete infiltration curve according to DL approach
44
45
46
47
48
49
50
51
52
53
54
55
56
57
58
59
60

1 **Table 1** - Characteristics of the investigated sites
2

Site	Coordinates UTM	Elevation and slope	Land use	Soil type	Clay (%)	Silt (%)	Sand (%)	Soil texture (USDA)
Ciavolo, Marsala (Italy)	37°45'19.2" N, 12°33'53.5" E	105 m a.s.l. 4.4%	<i>Pinus pinaster</i> (30 years old),	<i>Typic Rhodoxeralf</i>	33.4	43.0	23.6	Clay-loam
Ciavolo, Marsala (Italy)	37°45'19.6 " N, 12°33'58.1" E	105 m a.s.l. 4.4%	Spontaneous annual grasses	<i>Typic Rhodoxeralf</i>	28.5	34.5	39.6	Clay-loam
Javea, Alicante (Spain)	38°48'10.6"N 0°11'23.4"E	98 m a.s.l. 0%	<i>Pinus halepensis</i> (40 years old)	<i>Lithic Rhodoxeralf</i>	40.8	43.3	15.7	Silty-clay
Javea, Alicante (Spain)	38°48'15.0"N 0°09'18.8"E	213 m a.s.l 5%	Burned pine forest under different post- fire treatments	<i>Lithic Rhodoxeralf</i>	11.1	34.8	54.1	Sandy-loam

Table 2 – Means and coefficients of variation (CV) of initial soil water content, θ_i , bulk density, ρ_b , organic matter content, OM, and Water Drop Penetration Time, WDPT, for the experimental conditions considered resulting from different vegetation habitat (P = *Pinus pinaster* forest, H = *Pinus halepensis* forest; B = burned pine forest, G = glade), soil sampled horizon (O = organic soil, M = mineral soil), initial soil moisture condition (i.e., dry (D) or wet (W)) and post-fire treatment (no treatment (N), cutting treatment (C), and residues treatment (R)). Range between minimum and maximum values for WDPT is also given.

Experimental condition	θ_i (cm ³ cm ⁻³)			ρ_b (g cm ⁻³)			OM (%)			WDPT (s)			
	N	mean	CV (%)	N	mean	CV (%)	N	mean	CV (%)	N	geometric mean	CV (%)	Range
P-O-D	10	0.128	16.9	10	0.725	32.4	10	20.0	7.04	30	1689	48	868 - 3534
P-O-W	10	0.175	8.01	10	0.749	9.50	10	21.5	1.07	30	1454	182	150 - 6890
P-M-D	9	0.166	6.33	9	1.172	4.14	10	4.66	2.41	29	300	54	113 - 855
P-M-W	10	0.169	5.80	10	1.089	5.70	10	3.93	3.11	30	745	137	100 - 4425
G-M-W	10	0.281	7.51	10	1.192	4.73	10	4.71	6.02	29	<5	-	-
H-O-D	10	0.066	36.9	10	0.548	45.5	10	26.6	12.6	30	2139	116	480 - 7517
H-M-D	8	0.098	29.2	8	1.082	14.9	10	8.54	3.83	29	5	106	1 - 18
B-M-N	5	0.046	39.9	5	1.025	12.6	9	7.70	14.6	30	90	238	8 - 2220
B-M-C	5	0.020	19.3	5	0.876	19.4	9	6.73	13.6	30	45	951	5 - 1800
B-M-R	5	0.034	15.3	5	1.011	8.00	9	7.15	9.55	30	27	683	5 - 1200

Table 3 – Mean values of time to achieve steady state, t_s , steady state infiltration rate, i_s , and ethanol sorptivity, S_e , estimated according to different approaches from MDI tests conducted under different experimental conditions.

Experimental condition	N	t_s (h)	i_s (mm h ⁻¹)	Sorptivity, S_e (mm h ^{-0.5})			
				S1	SL	CL	DL
P-O-D	10	0.021	624.1	104.4	79.9	34.8	38.1
P-O-W	10	0.051	402.4	33.0	26.9	9.5	8.0
P-M-D	10	0.119	219.2	51.4	44.3	13.6	15.5
P-M-W	10	0.055	293.1	48.4	36.1	13.7	17.3
G-M-W	10	0.102	175.4	33.0	33.8	15.4	12.2
H-O-D	10	0.137	107.2	25.5	23.6	14.2	11.5
H-M-D	10	0.108	100.7	27.8	24.0	16.9	16.2
B-M-N	5	0.103	106.7	33.0	27.2	20.4	24.9
B-M-C	5	0.120	122.8	41.2	36.6	29.1	28.9
B-M-R	5	0.087	166.6	46.1	41.6	29.2	30.1
All data	N	85	85	85	85	84	84
	Min	0.01	45.1	10.2	10.9	0.4	0.7
	Max	0.27	1065	163.0	128.4	61.7	68.4
	Mean	0.09	249.4	45.1a	37.8b	18.6c	19.0c
	CV (%)	72.1	80.9	67.5	60.4	71.3	74.2

Mean values followed by the same letter are not statistically different according to a paired t-test ($P = 0.05$)

Table 4 – Mean values of duration, t_{tot} , infiltration rate, \bar{i} , and water sorptivity, S_w , estimated according to different approaches from MDI tests conducted under different experimental conditions.

Experimental condition	N	t_{tot} (h)	\bar{i} (mm h ⁻¹)	Sorptivity, S_w (mm h ^{-0.5})			
				S1	SL	CL	DL
P-O-D	10	7.10	7.0	5.4	2.7	1.7	1.5
P-O-W	10	4.18	12.6	6.9	8.1	4.9	3.5
P-M-D	10	2.47	24.8	6.8	3.1	1.6	1.1
P-M-W	10	2.14	26.8	7.9	7.1	6.2	5.4
G-M-W	10	0.53	101.7	22.9	24.1	14.9	12.8
H-O-D	10	4.34	3.8	n.a.	2.0	0.8	1.3
H-M-D	10	0.41	126.6	42.8	37.9	33.7	33.0
B-M-N	5	0.86	44.4	10.0	9.0	6.6	4.2
B-M-C	5	1.38	17.5	9.4	9.0	6.8	5.8
B-M-R	5	1.78	19.0	5.1	6.9	5.2	5.7
All data	N	85	85	49	85	80	82
	Min	0.2	0.7	5.1	0.9	0.2	0.2
	Max	9.0	249.9	76.4	63.9	60.1	61.5
	Mean	2.7	40.4	18.0a	11.5b	9.0b	8.0b
	CV (%)	86.1	125.0	93.8	115.6	133.1	147.3

Mean values followed by the same letter are not statistically different according to a paired t -test ($P = 0.05$)

Table 5 – Mean values of RI (Tillman et al., 1989) calculated according to SL, CL and DL approaches for the experimental conditions considered.

	RI_{SL}	RI_{CL}	RI_{DL}
P-O-D	55.1a	45.4a	52.3a
P-O-W	32.5a	19.5b	28.5ab
P-M-D	6.1a	1.9b	3.6a
P-M-W	9.7a	3.6b	4.6b
G-M-W	2.7a	2.0b	1.7b
H-O-D	22.4a	18.9a	19.3a
H-M-D	1.3a	1.0b	1.0b
B-M-N	6.6a	6.6a	12.8b
B-M-C	8.0a	8.3ab	10.5b
B-M-R	11.1a	10.4a	10.5a

Mean values on a row followed by the same letter are not statistically different according to HSD Tukey test ($P = 0.05$)

Table 6 – Statistics of the new repellency index RI_s (eq. 2) calculated according to CL and DL approaches for the experimental conditions considered.

	RI_{s-CL}					RI_{s-DL}				
	N	min	max	Geometric mean	CV (%)	N	min	max	Geometric mean	CV (%)
P-O-D	10	1.8	107.8	37.9a	92.4	10	1.3	99.1	39.3a	80.9
P-O-W	10	5.5	47.3	18.9a	63.9	10	2.7	59.6	21.1a	96.1
P-M-D	10	2.9	11.4	7.1a	38.6	10	3.9	27.4	12.1b	55.1
P-M-W	10	2.9	24.3	10.2a	64.7	10	3.7	22.4	11.7a	61.7
G-M-W	10	1.3	3.2	2.3a	22.4	10	1.4	4.0	2.7a	27.4
H-O-D	10	2.0	10.3	3.6a	68.8	10	0.7	8.5	4.0a	59.9
H-M-D	10	1.1	5.2	2.4a	61.6	10	0.9	3.1	1.9a	37.9
B-M-N	4	1.2	11.8	5.7a	91.5	4	1.5	4.5	2.4a	59.9
B-M-C	5	1.4	3.0	1.8a	38.2	5	1.4	7.8	3.5a	75.1
B-M-R	5	1.0	1.4	1.2a	12.8	5	1.0	2.0	1.7b	24.6

For a given experimental condition, mean values followed by the same letter are not statistically different according to a paired t-test ($P = 0.05$)

Table 7 – Coefficients of determination for linear regressions between the repellency index, RI_s (eq. 2), calculated according to both the CL and DL approaches and the repellency index, RI and the Water Drop Penetration Time, WDPT, for the experimental conditions considered ($N = 10$)

	R^2	P
RI_s CL vs. RI CL	0.753	**
RI_s CL vs. RI DL	0.805	**
RI_s CL vs. WDPT	0.378	*
RI_s DL vs. RI CL	0.730	**
RI_s DL vs. RI DL	0.763	**
RI_s DL vs. WDPT	0.459	*

* significant at $P = 0.05$; ** significant at $P = 0.01$

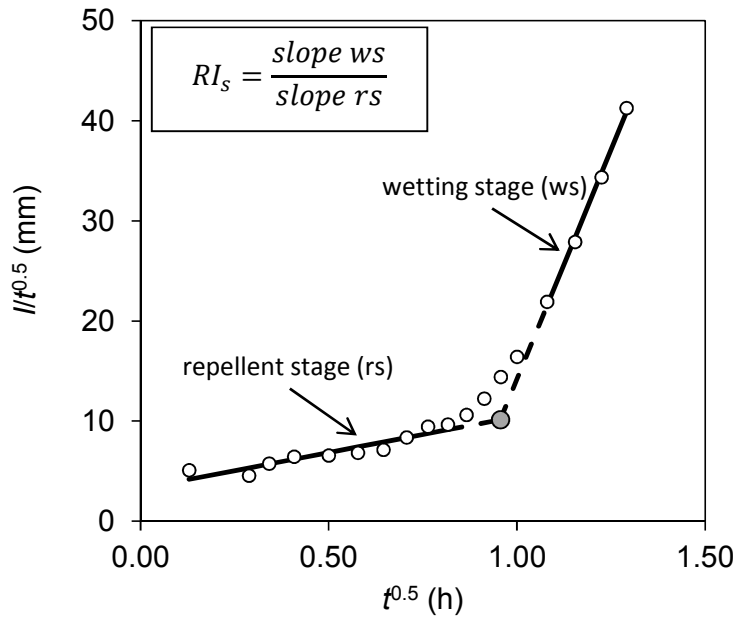


Figure 1 – Selection of the water repellent and wetting stages from linearized infiltration data (CL method).

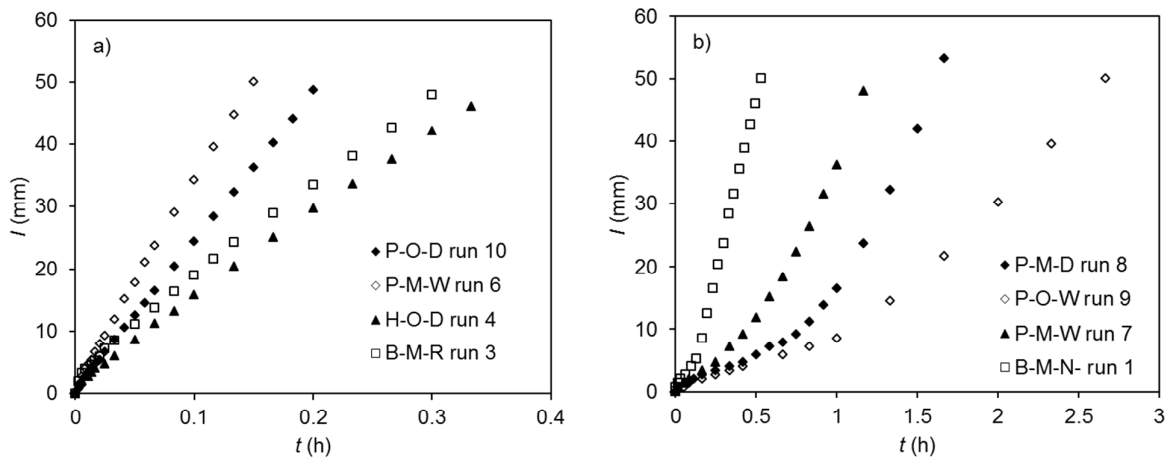


Figure 2 – Example of cumulative infiltration curves obtained in selected sites using a) ethanol and b) water as infiltrating fluid

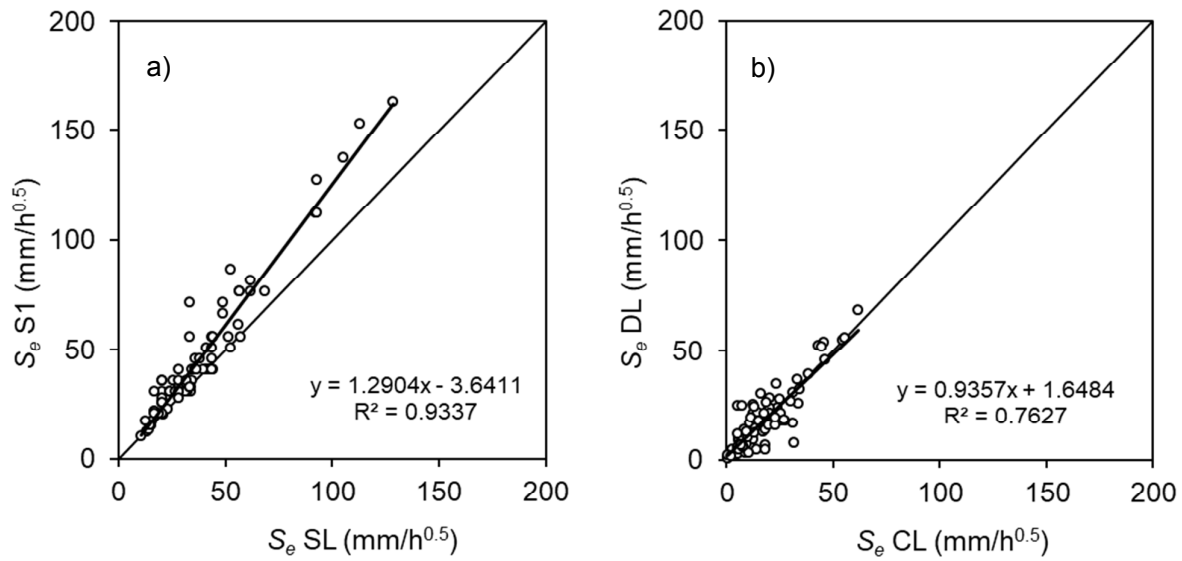


Figure 3 – Comparison between ethanol sorptivity values, S_e , estimated according to different approaches: a) SL vs. S1, b) CL vs. DL

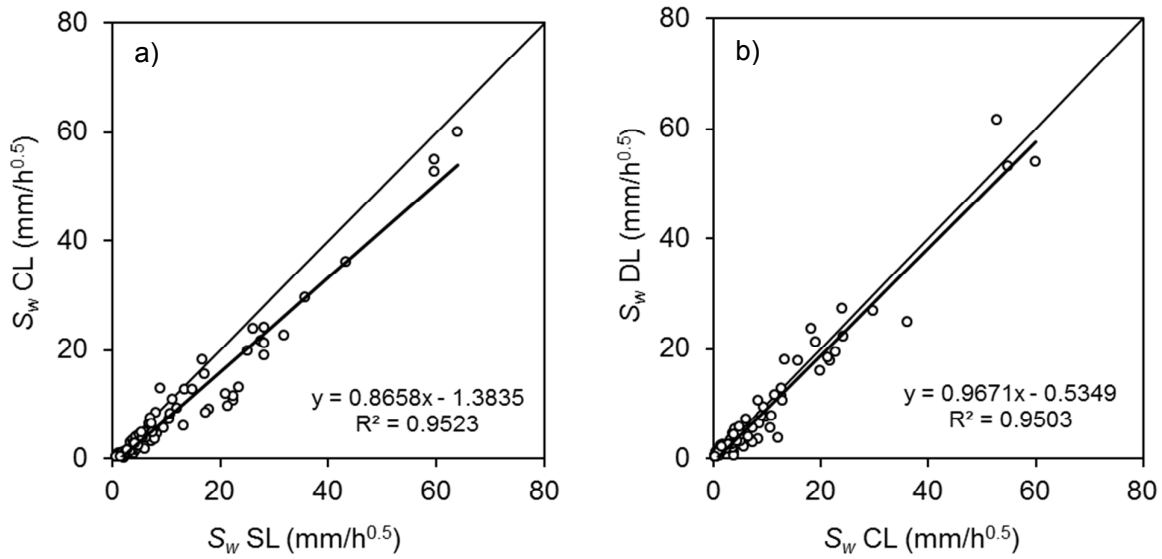


Figure 4 – Comparison between water sorptivity values, S_w , estimated according to different approaches: a) SL vs. CL, b) CL vs. DL

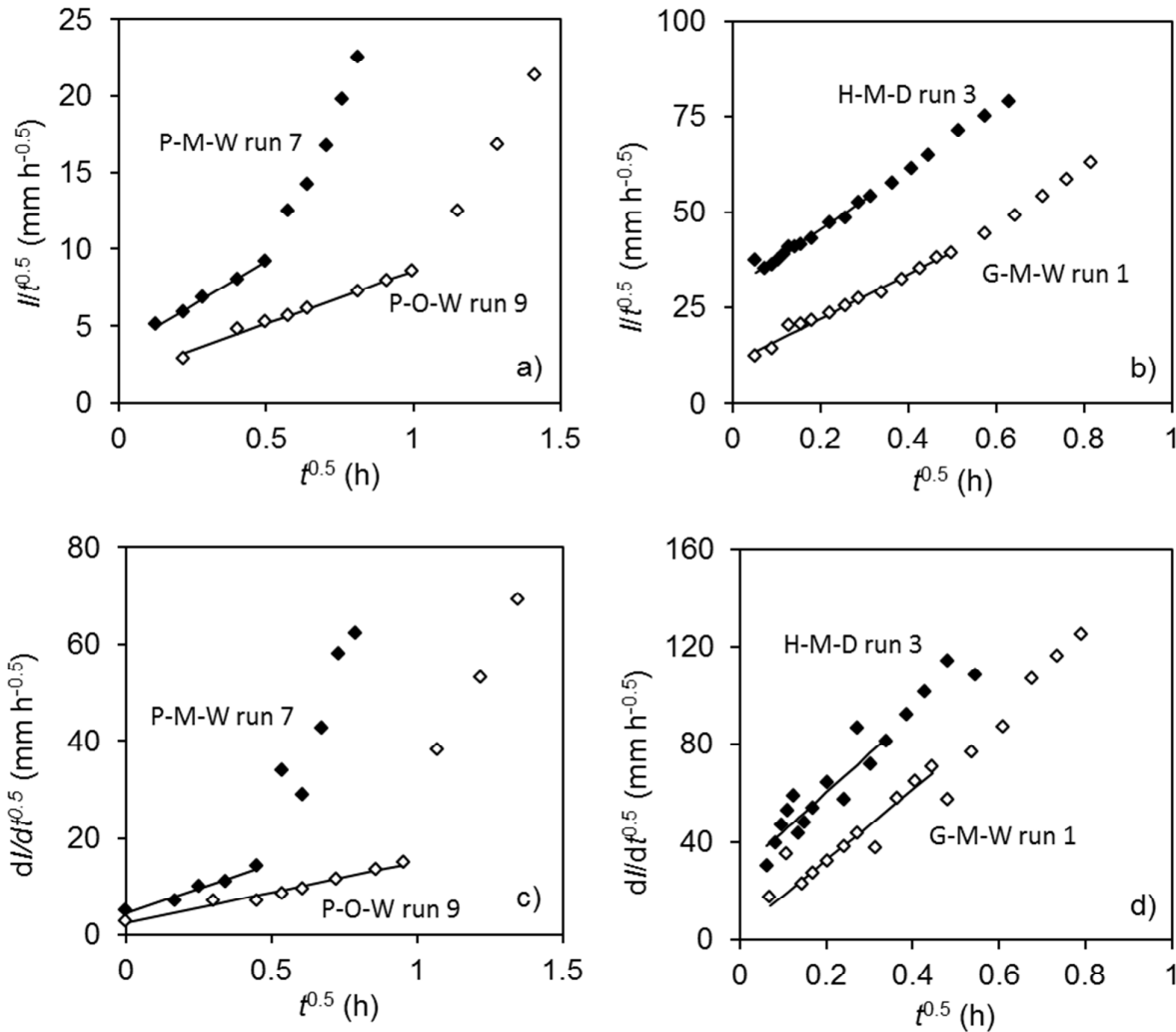
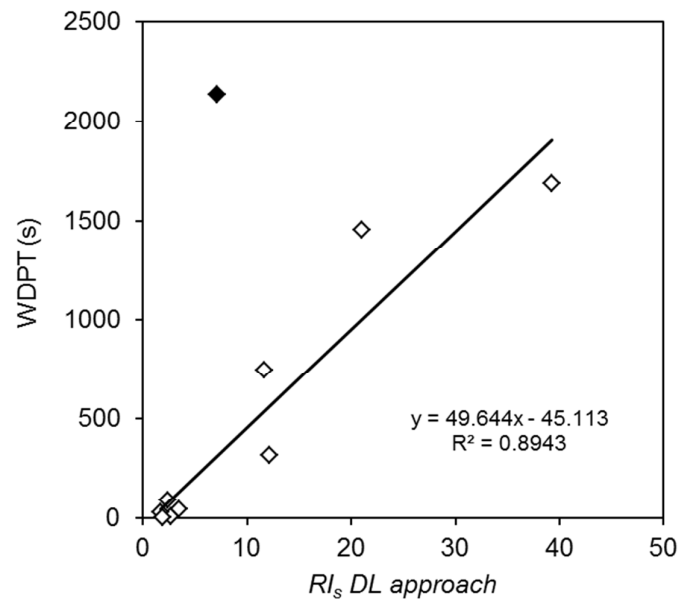


Figure 5 – Examples of application of cumulative linearization CL approach (a and b) and differentiated linearization DL approach (c and d) to water infiltration experiments in hydrophobic (a and c) and non-hydrophobic (b and d) soils

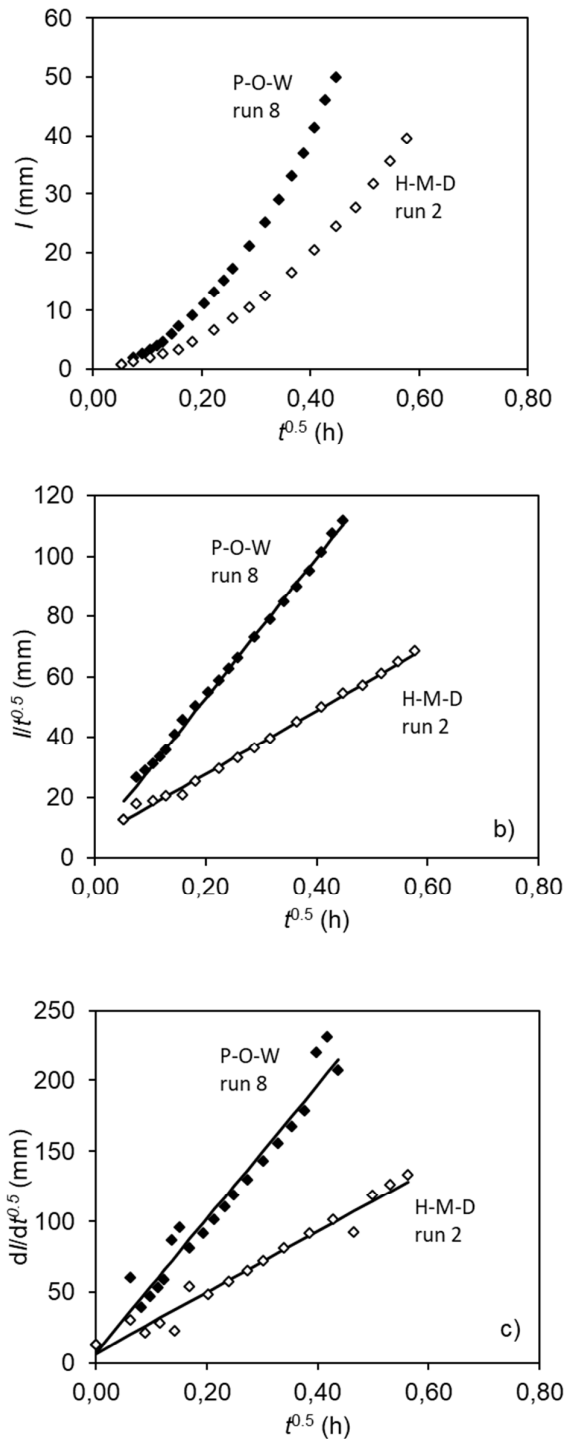


3

4 **Figure 6** – Relationship between the repellency index RI_s calculated by the DL approach and the
 5 Water Drop Penetration Time (WDPT) for the different experimental conditions considered ($N = 9$).
 6 Filled dot refers to the data collected in the organic layer of Javea forest site (H-O-D) that was
 7 excluded from the regression analysis.

8

9



1

2 **Figure 7** – Examples of cumulative ethanol infiltration curves plotted according to different
 3 representations: a) linearization of the early time infiltration data in the form I vs. $t^{0.5}$; b)
 4 linearization of the complete infiltration curve according to CL approach; c) linearization of the
 5 complete infiltration curve according to DL approach

1